The von Neumann Triple Point Paradox

Richard Sanders[1][*] and Allen M. Tesdall[2][†]

[1] Department of Mathematics, University of Houston, Houston, TX 77204, USA
   sanders@math.uh.edu
[2] Fields Institute, Toronto, ON M5T 3J1, Canada and Department of
   Mathematics, University of Houston, Houston, TX 77204, USA
   atesdall@fields.utoronto.ca

Summary. We describe the problem of weak shock reflection off a wedge and discuss the triple point paradox that arises. When the shock is sufficiently weak and the wedge is thin, Mach reflection appears to be observed but is impossible according to what von Neumann originally showed in 1943. We summarize some recent numerical results for weak shock reflection problems for the unsteady transonic small disturbance equations, the nonlinear wave system, and the Euler equations. Rather than finding a standard but mathematically inadmissible Mach reflection with a shock triple point, the solutions contain a complex structure: there is a sequence of triple points and supersonic patches in a tiny region behind the leading triple point, with an expansion fan originating at each triple point. The sequence of patches may be infinite, and we refer to this structure as Guderley Mach reflection. The presence of the expansion fans at the triple points resolves the paradox. We describe some recent experimental evidence which is consistent with these numerical findings.

Key words: self-similar solutions, two-dimensional Riemann problems, triple point paradox

1 Introduction

Consider a planar normal shock in an inviscid compressible and calorically perfect gas which impinges on a fixed wedge with apex half angle θ_w, see Figure 1. Given an upstream state with density $\rho = \rho_r$, velocity $u = v = 0$ and pressure $p = p_r$, one calculates that downstream of a *fast* (i.e., $u + c$) shock
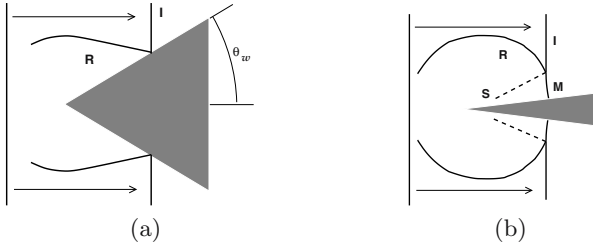
Fig. 1. A planar shock moving from left to right impinges on a wedge. After contact, I indicates the incident shock and R indicates the reflected shock. On the right, the dotted line S indicates a slip line and M is the Mach stem. Regular reflection is depicted on the left. Irregular reflection is depicted on the right.
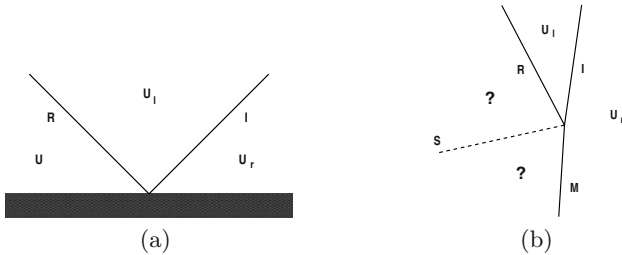

Fig. 2. A blow-up of the incident and reflected shock intersection. Regular reflection is on the left and irregular on the right. The constant states upstream and downstream of the incident shock are denoted by U_r and U_l. Whether or not constant states indicated by the question marks exist depends on the strength of I.

$$\frac{p_l}{p_r} = \frac{2\gamma}{\gamma+1} M^2 - \frac{\gamma-1}{\gamma+1}, \quad \frac{u_l}{c_r} = \frac{2}{\gamma+1}\left(M - \frac{1}{M}\right),$$
$$\frac{\rho_l}{\rho_r} = \frac{(\gamma+1)\, M^2}{2 + (\gamma-1)\, M^2}, \tag{1}$$

where γ denotes the ratio of specific heats, and $M > 1$ denotes the shock Mach number defined as the Rankine–Hugoniot shock speed divided by the upstream speed of sound $c_r = \sqrt{\gamma p_r/\rho_r}$. Following interaction, a number of self-similar (with respect to the wedge apex) reflection patterns are possible, depending on the values of M and θ_w.

This wedge reflection problem has a rich history, experimentally, analytically, and numerically. Probably the earliest and most significant analytical result was found by von Neumann [Neu43]. In this work were first formulated the equations which describe two and three planar shocks meeting at a point separated by constant states, see Figure 2. The two shock theory leads to what is known as *regular reflection*. The three shock theory leads to *Mach reflection*. For supersonic regular reflection, state U immediately behind the reflected shock R is supersonic and becomes subsonic across a sonic line downstream (toward the wedge's apex). When the incident shock angle is increased

to $\pi/2 - \theta^*(M)$ with respect to the wall, where $\theta_w = \theta^*(M)$ is the critical wedge half angle, state U becomes sonic. Therefore, at $\theta_w = \theta^*(M)$, acoustic signals generated downstream (e.g., from the wedge apex) will overtake the R-I reflection point, conceivably causing transition from regular reflection, depicted in the left figure, to irregular reflection, depicted in the right figure. This is one of several criteria which have been suggested to explain transition from regular to irregular reflection; see Henderson [Hen87] for a thorough and detailed discussion.

Loosely speaking, a *weak* incident shock has M slightly larger than 1, whereas a *strong* incident shock has M substantially larger than one. Theoretical analysis indicates that transition to Mach reflection is impossible when the incident shock is sufficiently weak. In fact, triple point solutions, as depicted in Figure 2(b), do not exist for sufficiently weak shocks. However, experiments in which weak shock waves are reflected off a wedge with $\theta_w \ll \theta^*(M)$ appear to show a standard Mach reflection pattern. This apparent disagreement between theory and experiment was discussed by von Neumann and has since become known as the von Neumann triple point paradox [Neu63, Hen87, SA05].

Guderley [Gud47, Gud62] as far back as 1947 proposed that there is an expansion fan and a supersonic region directly behind the triple point in a steady weak shock Mach reflection. He demonstrated that one could construct local solutions consisting of three plane shocks, an expansion fan, and a contact discontinuity or slip line meeting at a point. However, despite intensive experimental [BT49, STS92, Ste59] and numerical [CH90, BH92, TR94] studies, no evidence of an expansion fan or supersonic patch was observed. The first evidence supporting Guderley's proposed resolution was contained in numerical solutions of shock reflection problems for the unsteady transonic small disturbance equations in [HB00] and the compressible Euler equations in [VK99]. There were presented solutions that contain a tiny supersonic region embedded in the subsonic flow directly behind the triple point in a weak shock Mach reflection. Subsequently, Zakharian et al. [ZBHW00] found a supersonic region in a numerical solution of a shock reflection problem for the Euler equations, for a set of parameter values corresponding to those used in the unsteady transonic small disturbance solution in [HB00]. The supersonic region in the solutions in [VK99, HB00, ZBHW00] is extremely small, which explains why it had not been observed earlier.

This paper is organized as follows. In Section 2 the unsteady transonic small disturbance asymptotic model for a weak shock impinging on a thin wedge is recalled. Numerical evidence is offered to suggest an interesting resolution of the von Neumann paradox. Experimental evidence to support what was found numerically is displayed at the end of this section. In Section 3 a simple 3×3 hyperbolic system is given which exhibits irregular reflection but does not admit Mach reflection. It is solved numerically, displaying very similar structure to what was found in Section 2. Finally, the full compressible Euler equations are solved in Section 4 for a very weak incident shock

impinging on a thin wedge. The numerical solution appears to be in agreement
with what is found for the model problems from the previous sections.

2 The Weak Shock Thin Wedge Limit

The compressible Euler equations are given by

$$\frac{\partial \rho}{\partial t} + \nabla \cdot \rho \mathbf{u} = 0,$$

$$\frac{\partial \rho \mathbf{u}}{\partial t} + \nabla \cdot \rho \mathbf{u} \otimes \mathbf{u} + \nabla p = 0, \tag{2}$$

$$\frac{\partial \rho e}{\partial t} + \nabla \cdot (\rho e + p)\mathbf{u} = 0,$$

where ρ is the fluid density, $\mathbf{u} = (u, v)$ is the x-y velocity vector, p is the
pressure and e is the total energy per unit mass. The internal energy per unit
mass $\varepsilon = e - 1/2|\mathbf{u}|^2$, and we take $p = (\gamma - 1)\rho\varepsilon$ for a calorically perfect gas
with the constant ratio of specific heats $\gamma > 1$.

Consider an incident planar shock with Mach number $M = 1 + \varepsilon^2$ striking
a thin wedge with half angle $\theta_w = a\varepsilon$, where $\varepsilon > 0$ is destined to vanish. Take
the undisturbed upstream state U_r as $\rho = \rho_r$, $u = v = 0$ and $p = p_r$, yielding
an upstream speed of sound $c_r = \sqrt{\gamma p_r/\rho_r}$. From (1), calculate that U_l is

$$\frac{p_l}{p_r} = \left(1 + \frac{4\gamma}{\gamma + 1}\varepsilon^2\right) + O(\varepsilon^4), \qquad \frac{u_l}{c_r} = \frac{4}{\gamma + 1}\varepsilon^2 + O(\varepsilon^4),$$

$$\frac{\rho_l}{\rho_r} = \left(1 + \frac{4}{\gamma + 1}\varepsilon^2\right) + O(\varepsilon^4), \qquad \frac{v_l}{c_r} = \frac{-4}{\gamma + 1}a\varepsilon^3 + O(\varepsilon^5). \tag{3}$$

Hunter and Brio [HB00] observed the scales shown in (3) and proposed an
asymptotic model based on

$$p = p_r(1 + \varepsilon^2 \hat{p}), \qquad u = c_r\varepsilon^2 \hat{u},$$
$$\rho = \rho_r(1 + \varepsilon^2 \hat{\rho}), \qquad v = c_r\varepsilon^3 \hat{v},$$

and the stretched independent variables

$$\hat{x} = \frac{x - p(t)}{\varepsilon^2}, \qquad \hat{y} = \frac{y}{\varepsilon},$$

where $p(t)$ is the location where the incident shock would (neglecting possible
interactions) strike the wedge wall at time t,

$$p(t) = c_r \cos(\theta_w)(1 + \varepsilon^2)\, t = c_r \cos(a\varepsilon)(1 + \varepsilon^2)\, t \approx c_r(1 - (1 - a^2/2)\varepsilon^2)\, t,$$
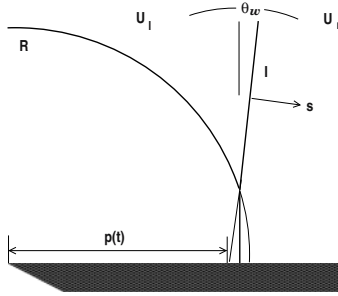
Fig. 3. A weak shock over a thin wedge. U_r and U_l are the states to the right and left of the incident shock I. $\theta_w = a\varepsilon \ll 1$ and the incident shock has Mach number $M = 1 + \varepsilon^2$. $x = p(t)$ is the location where I would intersect the wall at time t, neglecting interaction.

see Figure 3. Inserting these into (2), equating like powers of ε, and making an additional order one change of variable (denoted by $\breve{u}$, etc.), they find that $\breve{u}$ and $\breve{v}$ asymptotically satisfy

$$\breve{u}_t + \left(1/2\,\breve{u}^2\right)_{\breve{x}} + \breve{v}_{\breve{y}} = 0,$$
$$\breve{u}_{\breve{y}} - \breve{v}_{\breve{x}} = 0. \tag{4}$$

This is, of course, the celebrated *unsteady transonic small disturbance equation* (UTSDE). The UTSDE is solved on the upper half plane with a *no-flow* boundary condition $\breve{v}(\breve{x}, 0, t) = 0$ along $\breve{y} = 0$ and initial data

$$(\breve{u}(\breve{x}, \breve{y}, 0), \breve{v}(\breve{x}, \breve{y}, 0)) = \begin{cases} (0, 0) & \text{if } \breve{x} > \breve{a}\breve{y} \\ (1, -\breve{a}) & \text{if } \breve{x} < \breve{a}\breve{y}, \end{cases}$$

where

$$\breve{a} = \frac{a}{2} = \frac{1}{2} \frac{a\varepsilon}{\sqrt{1 + \varepsilon^2 - 1}} \sim \frac{1}{2} \frac{\theta_w}{\sqrt{M - 1}}.$$

The jump at $\breve{x} = \breve{a}\breve{y}$ corresponds to the incident shock I. The data is vorticity-free but incompatible with the no-flow boundary condition behind. As time advances, the reflected wave pattern R will emerge from the trailing boundary.

For $\breve{a}$ in the range $0 < \breve{a} < \sqrt{2}$, regular reflection for this initial-boundary value problem is impossible [BH92]. Moreover, it is shown in [BH92] as well as in [TR94] that (4) can never admit triple point solutions. Therefore, this asymptotic model equation is very well designed to investigate the von Neumann triple point paradox.

A numerical solution to (4) was obtained in [HB00] for the value $\breve{a} = 0.5$ (a value for which regular reflection does not occur). An irregular reflection pattern globally resembling single Mach reflection was observed. When the region containing the apparent triple point was greatly refined, however, a small supersonic patch located in the subsonic zone directly below the reflected shock and behind the Mach stem was detected, see [HB00, page 242]. This,

along with the contemporaneous work in [VK99], was the first indication that Guderley's resolution of the triple point paradox might be essentially correct. Using a new numerical scheme, a subsequent study by Tesdall and Hunter [TH02], we further investigated the structure of irregular reflection found in the UTSDE asymptotic model.

The supersonic patch detected in [VK99, HB00] appeared to confirm Guderley's four-wave solution. The patch indicates that it is plausible for an expansion wave to be a (unobserved) part of the observed three shock confluence. We briefly summarize the numerical techniques employed by Tesdall and Hunter. First, they used a parabolic grid aligned with the weak reflected shock. They then solved the UTSDE in self-similar variables $\check{x} \to \check{x}/t, \check{y} \to \check{y}/t$. The advantage of using self-similar coordinates is that the problem remains fixed on the computational grid, and a steady self-similar solution is obtained by letting a pseudo-time $t \to \infty$. Following the classical Cole–Murman approach, $(\check{u}, \check{v})$ is written as $\operatorname{grad}\phi$. The nonlinearities in the resulting scalar equation are discretized by a min-mod limited Engquist–Osher numerical flux. A steady state solution is obtained by lagged implicit time marching and grid continuation.

We present results obtained by the method of Tesdall and Hunter in Figure 4. The full simulation is carried out on a spatial grid that fits in $[-3, 2] \times [0, 2.5]$, with the inverse slope parameter $\check{a} = 0.5$. The total number of grid points employed is approximately 2.7×10^6, where, by local grid refinement, the region depicted in Figure 4(a) spans $768 \times 608 \approx 4.7 \times 10^5$ points. This yielded a grid size near the triple point of approximately 1.5×10^{-5}.

Clear evidence of an expansion fan is seen at the triple point depicted in Figure 4. What is equally remarkable is what appears to be a sequence of progressively smaller and weaker shock/expansion pairs running a short distance (less than 2%) down the length of the Mach stem. The expansion from wave i appears to terminate through its interaction with the shock from wave $i + 1$. The supersonic region behind the leading triple point is extremely small, which explains why it had not been observed earlier. The results in [TH02] suggest that the sequence of triple points and expansion waves/shocks in a weak shock irregular reflection may be infinite. Whether this sequence is infinite or not is certainly impossible for any numerical simulation to determine. In fact, one could argue that the structure indicated in Figure 4 may be numerical flux dependent (upwind/non-upwind) or that the asymptotic model may predict something that is not physically realized. We address these concerns here and in the following sections.

Experimental confirmation poses a most challenging problem simply because the computed *Guderley Mach reflection* structure is so small and weak. Nevertheless, some experimental evidence has recently been obtained. Following the announcement of the Guderley Mach reflection solution found in [TH02], Skews and Ashworth [SA05] modified an existing shock tube experimental apparatus in order to obtain Mach stem lengths more than an order of magnitude larger than those possible from conventional shock tubes. All
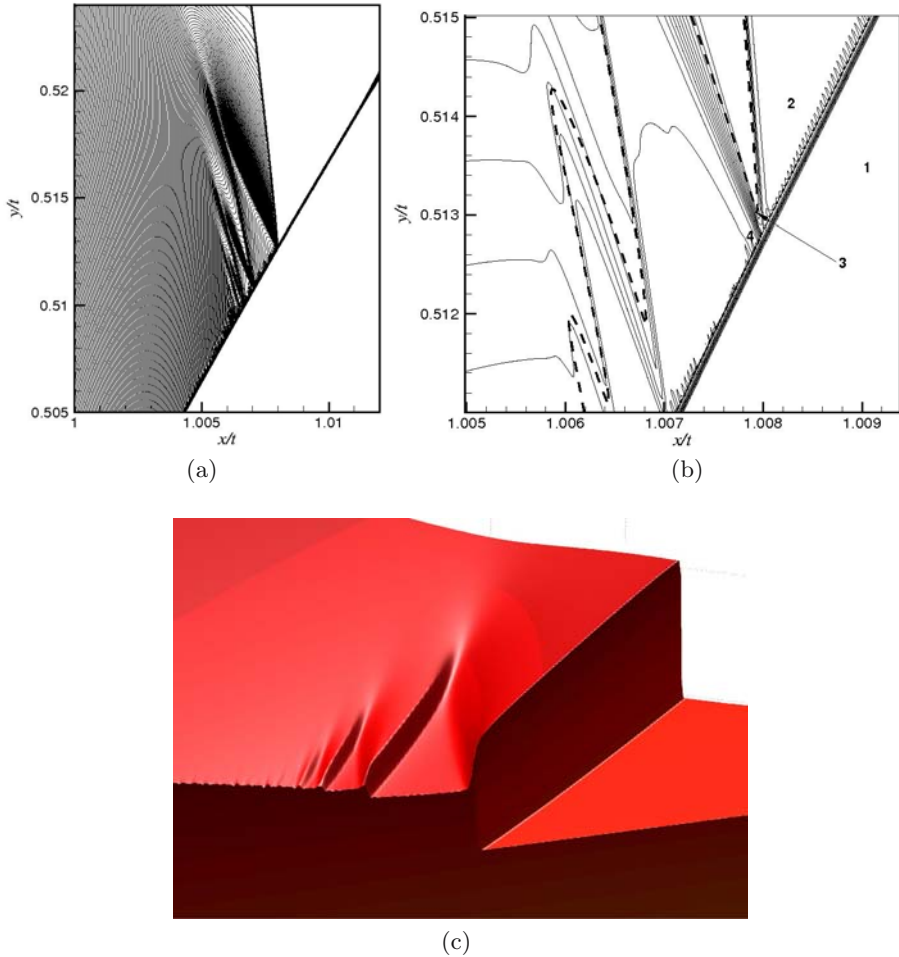
(a)

(b)

(c)

Fig. 4. Closeups of an apparent triple point for the UTSDE using the approach of Tesdall and Hunter. In (a) and (b) the incident shock leaves to the upper right, the reflected shock towards the top, and the Mach stem exits at the bottom. The plot in (a) depicts contour lines of u and shows a sequence of expansions/shocks running down the Mach stem. The plot in (b) shows a detail of v; 1 denotes state $v = 0$, 2 state $v = -\breve{a}$ and 3 points to the expansion wave emanating from what appears macroscopically to be a triple point. The dotted line in (b) delineates the supersonic patches within the subsonic zone behind the Mach stem. The *Guderley Mach reflection* structure can be seen better in the surface plot (c) where the viewer is upstream looking back at the triple point.

experiments were carried out on a 15° ramp with incident shock Mach numbers ranging from 1.05 to 1.1. They present images that "clearly show the existence of an expansion wave immediately behind the reflected wave as proposed by Guderley", and they found "a distinct sharp contrasting line immediately

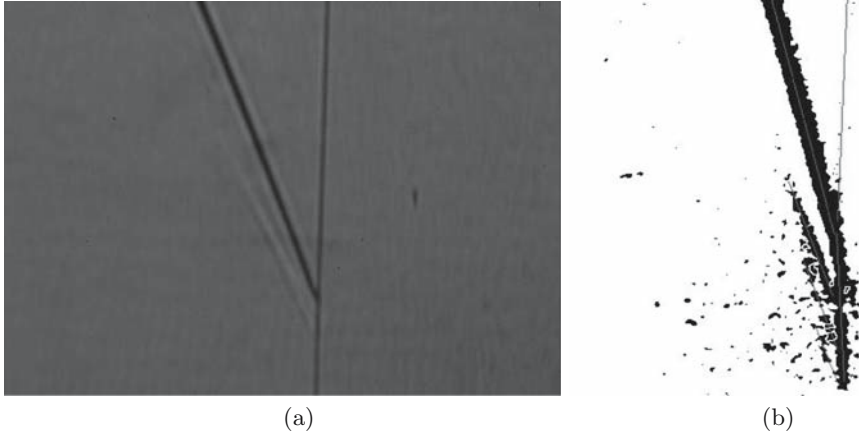(a)   (b)

Fig. 5. On the left, a schlieren image of an experimental weak shock reflection. The incident shock (vertical) exits at the top and is moving from left to right. The reflected wave exits to the upper left, and an expansion wave is visible immediately behind it. A highly contrasted image is on the right, showing evidence of a second shocklet behind the first.

after the expansion wave, indicating the existence of a terminating shock". In addition, they obtained evidence in some of their images of a second terminating shocklet behind the first, as predicted by the simulations in [TH02]. Professor Beric Skews graciously supplied us with the images which we give here in Figure 5. Further experimental refinements and data acquisition are currently underway.

3 The Nonlinear Wave System

Here we consider a problem for the nonlinear wave system which is analogous to the reflection of weak shocks discussed in the previous section. The shock reflection problem consists of the nonlinear wave system

$$\frac{\partial \rho}{\partial t} + \nabla \cdot \rho \mathbf{u} = 0,$$

$$\frac{\partial \rho \mathbf{u}}{\partial t} + \operatorname{grad} p = 0,$$

in the half space $x > 0$ with piecewise constant Riemann data consisting of two states separated by a discontinuity located at $x = \kappa y$. Again, ρ should be thought of as density, $\mathbf{u} = (u, v)$ as velocity having x- and y-components, and $p = p(\rho)$ as pressure. For convenience, we assume $p(\rho) = C\rho^\gamma$ where C is a constant and $\gamma = 2$. See [TSK06].

The nonlinear wave system is a simplification of the isentropic Euler equations obtained by dropping the momentum transport terms from the

momentum equations. Compared to the UTSDE, the nonlinear wave system is closer in structure to the Euler equations: it is linearly well-posed in space and time, it has a characteristic structure similar to the Euler equations with nonlinear acoustic waves coupled (weakly) to linearly degenerate waves, and it respects the spatial Euclidean symmetries of gas dynamics (excluding space-time Galilean symmetry, of course). In fact (see [KF94]), it may be the simplest system one can construct with these symmetries. It has also served as a prototypical model for the theoretical study of shock wave reflection [ČK98, ČKK05, ČKK01]. However, the greatest attribute of (3) for our purposes is the sheer simplicity of its wave structure. Moreover, the fluxes are quadratic (when $\gamma = 2$), and so its flux Jacobians are linear in conserved variables. The Jacobian's eigenvalues are 0 and $\pm c$, where $c = \sqrt{p_\rho}$, and it has extremely simple eigenvectors. It is very well suited for efficient finite differencing.

Let $U = (\rho, m, n)$ denote the vector of conserved variables, where $m = \rho u$ and $n = \rho v$, and consider the following two-dimensional Riemann data:

$$U(x, y, 0) = \begin{cases} U_1 \equiv (\rho_1, 0, 0) & \text{if } x < \kappa y, \\ U_0 \equiv (\rho_0, 0, n_0) & \text{if } x > \kappa y. \end{cases} \qquad (5)$$

We choose $\rho_0 > \rho_1$ to obtain an upward moving shock in the far field, and determine n_0 so that the one-dimensional wave between U_0 and U_1 at inverse slope κ consists of a shock and a contact discontinuity with a constant middle state between them. The following expression for n_0 is readily determined:

$$n_0 = \frac{1}{\kappa} \sqrt{(1 + \kappa^2)(p(\rho_0) - p(\rho_1))(\rho_0 - \rho_1)}. \qquad (6)$$

There is no physical wall in the Mach reflection simulation below. Rather, reflection occurs because the vertical axis is a line of left-right symmetry, see Figure 6(a). Here, for κ sufficiently large ($\kappa = 1$ will do), regular reflection is impossible. Moreover, as with the UTSDE, (3) can never admit triple point solutions, see [TSK06]. So we now investigate the structure of irregular reflection, this time, however, for a hyperbolic system – one which resembles the Euler equations but is not obtained from them via a limit.

The essential feature of the numerical method employed is the capability to locally refine the grid in the area of the apparent triple point. We again use self-similar variables

$$x \rightarrow x/t \equiv \xi, \quad y \rightarrow y/t \equiv \eta$$

to cast the problem into one which remains fixed on the grid. Non-uniform, logically rectangular, finite volume grids are constructed so that for a given κ the incident shock is aligned with the grid in the far field. Specifically, each problem with a given incident shock angle has a set of associated finite volume C-grids, each grid in the set corresponds to a level of grid refinement, and we use these to *grid continue* to a steady state.
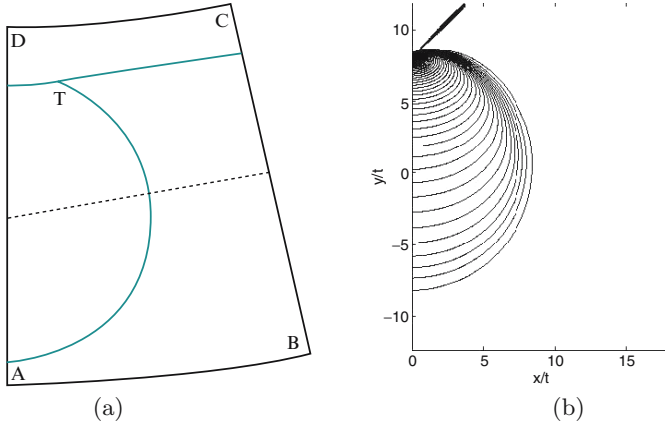
Fig. 6. A schematic diagram of the computational domain is on the left. AD is the line of symmetry. On the right is a computed self-similar solution with $\kappa = 1$.

The basic finite volume schemes used are quite standard. Each grid cell, Ω, is a quadrilateral and, using $\boldsymbol{\nu} = (\nu_\xi, \nu_\eta)$ to denote the normal vector to a typical side of Ω, numerical fluxes are designed to be consistent with

$$\widetilde{F}(U) = (F(U) - \xi U)\,\nu_\xi + (G(U) - \eta U)\,\nu_\eta = \begin{pmatrix} \nu_\xi m + \nu_\eta n - \bar{\xi}\,\rho \\ \nu_\xi p - \bar{\xi}\,m \\ \nu_\eta p - \bar{\xi}\,n \end{pmatrix},$$

where $\bar{\xi} = (\boldsymbol{\xi}\cdot\boldsymbol{\nu})$ and $\boldsymbol{\xi} = (\xi, \eta)$. Since $\boldsymbol{\xi}$ varies in space, numerical flux formulae are evaluated at $\boldsymbol{\xi}$ frozen at the midpoint of each cell side. Two distinctly different numerical fluxes are utilized in the results presented below:

1. Lax–Friedrichs:

$$H_{\mathrm{LF}} = \frac{1}{2}\left(\widetilde{F}(U_l) + \widetilde{F}(U_r) - \Lambda\,(U_r - U_l)\right),$$

where $\Lambda > 0$ is a scalar constant chosen to be larger than the fastest wave speed found on the computational domain.

2. Roe:

$$H_{\mathrm{Roe}} = \frac{1}{2}\left(\widetilde{F}(U_l) + \widetilde{F}(U_r) - R\Lambda L\,(U_r - U_l)\right),$$

where $\Lambda = \mathrm{diag}(|-\bar{\xi} - c|, |-\bar{\xi}|, |-\bar{\xi} + c|)$, and R and L are the matrices of the right and left eigenvectors to the Jacobian of $\widetilde{F}$ evaluated at the midpoint $U_{\mathrm{Roe}} = \frac{1}{2}(U_l + U_r)$. Since we use the equation of state $p = 1/2\rho^2$, the midpoint yields an exact Roe average.

In order to investigate the structure of the solution near the triple point in a manner that has as little numerical bias as possible, we opted to first solve the problem using the classic first-order accurate Lax–Friedrichs finite
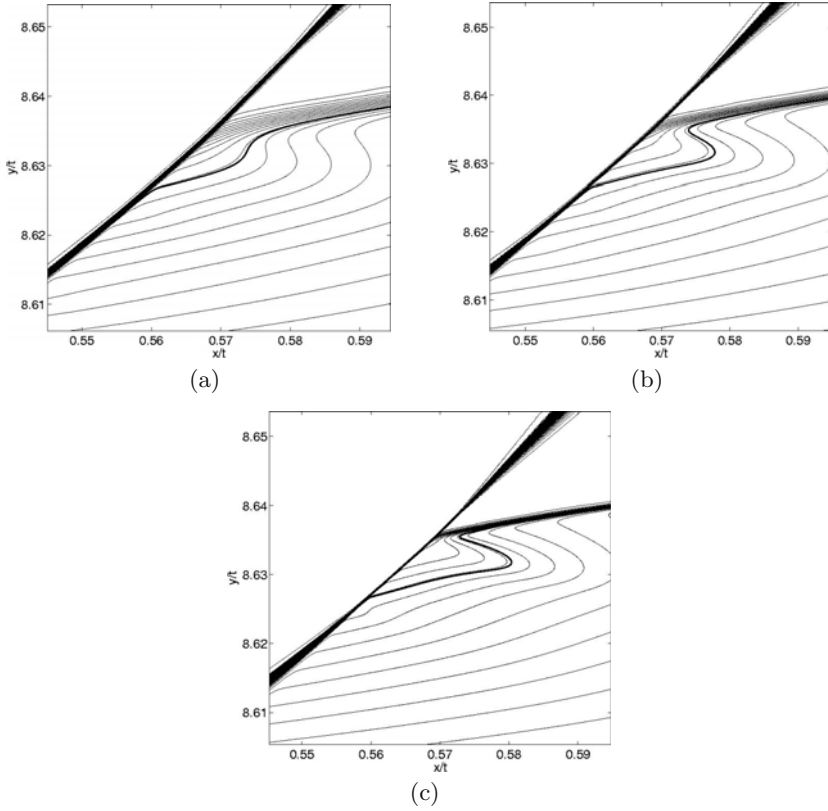
(a)

(b)

(c)

Fig. 7. Density contour plots for the nonlinear wave system using the first order accurate Lax–Friedrichs finite volume scheme in a neighborhood of the triple point. The region shown includes the locally refined 760×760 grid in (a), the 1280×1024 grid in (b) and the 2048×1320 grid in (c). The heavy line below the reflected shock and to the right of the Mach stem delineates a supersonic patch found within the subsonic zone. There is a slight indication of an expansion fan behind the leading triple point in (c).

volume scheme. That is, the Lax–Friedrichs flux is used in conjunction with piecewise constant cell-wise reconstruction. Figure 7 depicts a closeup of what was found on three grids with increasing refinement. The largest grid (c) contains approximately 11 million grid points. Approximately one quarter of these are contained in a square of length 0.05 units centered on the triple point. The solution in (c) clearly resolves a small patch of supersonic flow behind the triple point. This patch is quite small with width of approximately 0.03 and height of approximately 0.01. Note the fattening of the incident and Mach shocks as they leave the region of extreme grid refinement. The much weaker reflected shock is well resolved since it is aligned with the grid, and the grid in the direction normal to the reflected shock is very fine near the triple point.
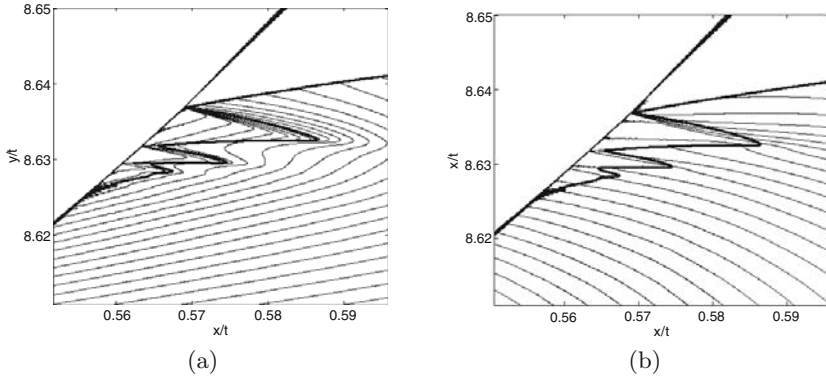
Fig. 8. Density contours (a) and x-momentum contours (b) for the nonlinear wave system using a high-order Roe scheme. These were obtained on the same grid depicted in Figure 7(c). There is now clear evidence of the sequence of interacting shocks and expansions seen earlier for the UTSDE. The heavy line is the sonic line and again delineates the supersonic patch.

The width of the supersonic patch is approximately 5% of the length of the Mach stem. There is a slight indication of an expansion fan at the triple point, but at this level of grid refinement there is no evidence yet of the sequence of shocks and expansions seen in Figure 4.

There comes a time when the results from a first-order scheme are, at best, inadequate, because of hardware limitations. The large grid results just displayed used a grid whose smallest grid size was on the order of one millionth of the extent of the computational domain. Moreover, these problems are steady and, therefore, require hundreds of thousands of pseudo-time iterations. At this stage we, therefore, employed a (perhaps) somewhat less unbiased numerical approach – a high-order scheme based on the Roe numerical flux. High-order accuracy is achieved by using a piecewise quadratic reconstruction limited in characteristic variables. We give the finest grid results from this approach in Figure 8. Three shock/expansion pairs are now clearly evident. The primary wave is at the triple point and two others can be seen along the Mach stem, a pattern very similar to that found for the UTSDE.

4 Weak Shock Irregular Reflection for the Euler Equations

We compute numerical solutions for the Euler equations (2) with $\gamma = 5/3$. A weak $M = 1.04$ vertically aligned incident shock impinges on a $\theta_w = 11.5°$ ramp. These data correspond to parameter $\breve{a} \approx 1/2$ in the UTSDE model from Section 2. The grid is defined by a conformal map of the form $z = w^\alpha$, and so it is orthogonal with a singularity at the ramp apex $x = y = 0$. The upstream speed of sound $c_r = 1$, and boundary data on the left, right and top is given
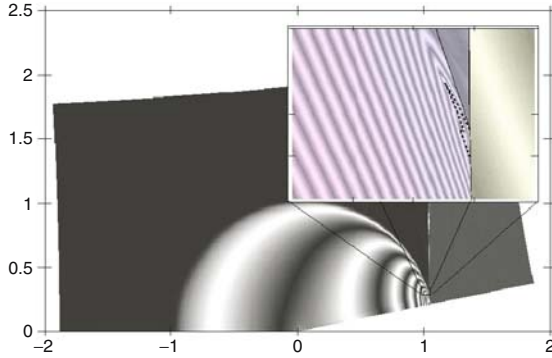
Fig. 9. The geometry of the $M = 1.04/11.5°$ Euler example. The insert indicates the region where extreme local grid refinement is performed.

to exactly agree with this shock located at $x = 1.04$. The lower boundary condition mimics symmetry about the x-axis for $x < 0$ and symmetry with respect to the ramp for $x > 0$. The grid geometry can be seen in Figure 9. This problem is well outside the range where regular reflection solutions are possible. Refer again to the figure to see that its numerical solution (under the insert) clearly resembles single Mach reflection. However, Mach reflection (where three plane shocks meet at a point) is also not possible for a shock this weak [Hen87]. This example demonstrates a classic von Neumann triple point paradox.

This problem is solved in self-similar coordinates by essentially the same high order Roe method discussed in the previous section. However, we simplify the Roe approach by again evaluating the Roe matrix at the midpoint, which for the Euler equations is only an approximation to the Roe average. Also, to avoid spurious expansion shocks, artificial dissipation on the order of $O(|U_r - U_l|)$ is appended to the diagonal part of the Roe dissipation matrix in a field by field manner.

We locally refine a very small neighborhood around the apparent triple point as done earlier. The full finest grid has eleven million grid points with $800 \times 2000 = 1.6 \times 10^6$ ($\Delta x \approx 5 \times 10^{-7}$) devoted to the local refinement. We plot the sonic number $\mathcal{M}$ which is defined as follows. The eigenvalue corresponding to a fast shock in unit direction $\mathbf{n}$ for the self-similar Euler flux Jacobian is

$$\lambda = (u - \xi, v - \eta) \cdot \mathbf{n} + c$$

where $\xi = x/t$ and $\eta = y/t$. Define $r^2 = \xi^2 + \eta^2$ and set $\mathbf{n} = (\xi, \eta)/r$, $u_n = (u, v) \cdot \mathbf{n}$ to find

$$\lambda = c\left(\frac{u_n - r}{c} + 1\right) = c(1 - \mathcal{M}) \quad \text{where} \quad \mathcal{M} = \frac{r - u_n}{c}.$$
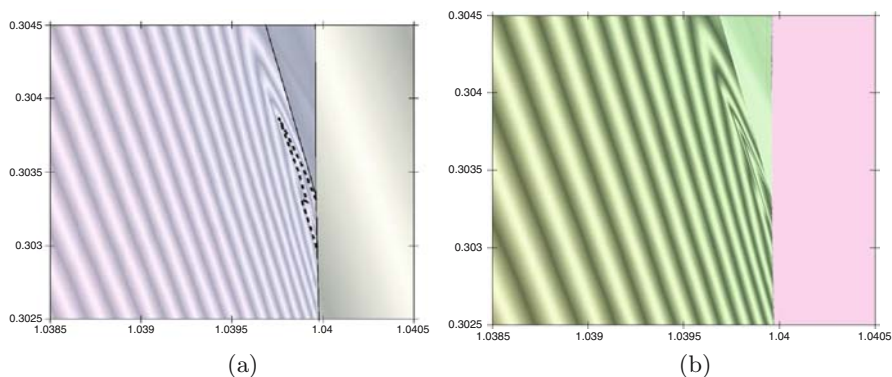
Fig. 10. A closeup of the Euler triple point. The sonic number $\mathcal{M}$ on the left and density ρ on the right. The dotted line on the left delineates the supersonic patch within the subsonic zone behind the Mach stem.
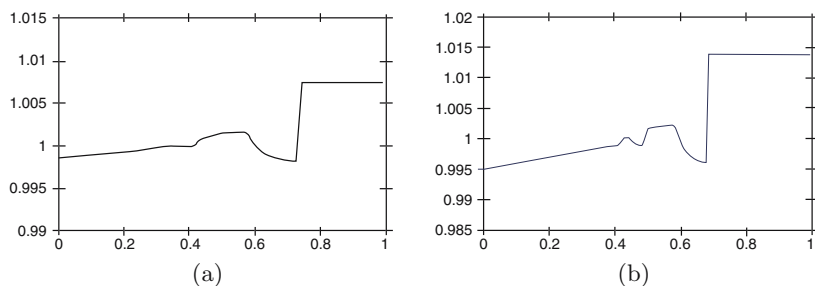

Fig. 11. Vertical cross sections of $\mathcal{M}$ taken bottom-up slightly to the left of the Mach stem. On the left $M = 1.04/11.5°$. The reflected shock is the large jump. Note the crossings at $\mathcal{M} = 1$. On the right, a second example problem with a slightly stronger incident shock $M = 1.075/15.0°$. The evidence of a sequence of shock/expansion wave pairs is stronger for this second example.

When $\mathcal{M} < 1$, the flow is called subsonic. When $\mathcal{M} > 1$, the flow is called supersonic. In this sense, when crossing through a self-similar stationary shock, the fact that $\mathcal{M}$ crosses from subsonic to supersonic is nothing more than the entropy condition $\lambda_l > s > \lambda_r$.

Figure 10 gives a sonic number contour plot (a) and density contours (b) in the triple point neighborhood. Clearly the evidence for Guderley Mach reflection in this example is not nearly as compelling as found for our earlier examples. However, these shocks are extremely weak. In recent work for a $\gamma = 7/5$ gas, we slightly strengthened the incident Mach number, $M = 1.075$, and obtained far more conclusive results. See the sonic number cross sections depicted in Figure 11.

References

[BH92]   M. Brio and J. K. Hunter. Mach reflection for the two-dimensional Burgers equation. *Phys. D*, 60:194–207, 1992.

[BT49]   W. Bleakney and A. H. Taub. Interaction of shock waves. *Rev. Modern Physics*, 21:584–605, 1949.

[CF76]   R. Courant and K. O. Friedrichs. *Supersonic Flow and Shock Waves*. Springer, 1976.

[CH90]   P. Colella and L. F. Henderson. The von Neumann paradox for the diffraction of weak shock waves. *J. Fluid Mech.*, 213:71–94, 1990.

[ČK98]   S. Čanić and B. L. Keyfitz. Quasi-one-dimensional Riemann problems and their role in self-similar two-dimensional problems. *Arch. Rational Mech. Anal.*, 144:233–258, 1998.

[ČKK01] S. Čanić, B. L. Keyfitz, and E. H. Kim. Mixed hyperbolic-elliptic systems in self-similar flows. *Bol. Soc. Bras. Mat.*, 32:1–23, 2001.

[ČKK05] S. Čanić, B. L. Keyfitz, and E. H. Kim. Free boundary problems for nonlinear wave systems: Mach stems for interacting shocks. *SIAM J. Math. Anal.*, 37:1947–1977, 2005.

[Gud47] K. G. Guderley. Considerations of the structure of mixed subsonic-supersonic flow patterns. Air Material Command Tech. Report, F-TR-2168-ND, ATI No. 22780, GS-AAF-Wright Field 39, U.S. Wright-Patterson Air Force Base, Dayton, Ohio, October 1947.

[Gud62] K. G. Guderley. *The Theory of Transonic Flow*. Pergamon Press, Oxford, 1962.

[HB00]   J. K. Hunter and M. Brio. Weak shock reflection. *J. Fluid Mech.*, 410:235–261, 2000.

[Hen66] L. F. Henderson. On a class of multi-shock intersections in a perfect gas. *Aero. Q.*, 17:1–20, 1966.

[Hen87] L. F. Henderson. Regions and boundaries for diffracting shock wave systems. *Z. Angew. Math. Mech.*, 67:73–86, 1987.

[HT04]   J. K. Hunter and A. M. Tesdall. Weak shock reflection. In D. Givoli, M. Grote, and G. Papanicolaou, editors, *A Celebration of Mathematical Modeling*. Kluwer Academic Press, New York, 2004.

[KF94]   B. L. Keyfitz and M. C. Lopes Filho. A geometric study of shocks in equations that change type. *J. Dynam. Differential Equations*, 6:351–393, 1994.

[Neu43] J. von Neumann. Oblique reflection of shocks. Explosives Research Report 12, Bureau of Ordinance, 1943.

[Neu63] J. von Neumann. *Collected Works, Vol. 6.* Pergamon Press, New York, 1963.

[Ric81] R. D. Richtmeyer. *Principles of Mathematical Physics, Vol. 1.* Springer, 1981.

[SA05]   B. Skews and J. Ashworth. The physical nature of weak shock wave reflection. *J. Fluid Mech.*, 542:105–114, 2005.

[Ste59] J. Sternberg. Triple-shock-wave intersections. *Phys. Fluids*, 2:179–206, 1959.

[STS92] A. Sasoh, K. Takayama, and T. Saito. A weak shock wave reflection over wedges. *Shock Waves*, 2:277–281, 1992.

[TH02]   A. M. Tesdall and J. K. Hunter. Self-similar solutions for weak shock reflection. *SIAM J. Appl. Math.*, 63:42–61, 2002.

[TR94]   E. G. Tabak and R. R. Rosales. Focusing of weak shock waves and the von Neumann paradox of oblique shock reflection. *Phys. Fluids*, 6:1874–1892, 1994.

[TSK06]   A. M. Tesdall, R. Sanders, and B. L. Keyfitz. The triple point paradox for the nonlinear wave system. *SIAM J. Appl. Math.*, 67:321–336, 2006.

[VK99]   E. Vasil'ev and A. Kraiko. Numerical simulation of weak shock diffraction over a wedge under the von Neumann paradox conditions. *Comput. Math. Math. Phys.*, 39:1335–1345, 1999.

[ZBHW00]   A. Zakharian, M. Brio, J. K. Hunter, and G. Webb. The von Neumann paradox in weak shock reflection. *J. Fluid Mech.*, 422:193–205, 2000.